Journal of Electroanalytical Chemistry 656 (2011) 72–77

Contents lists available at ScienceDirect

Journal of Electroanalytical Chemistry

journal homepage: www.elsevier.com/locate/jelechem

An electrochemical amperometric immunobiosensor for label-free detection of α-fetoprotein based on amine-functionalized graphene and gold nanoparticles modified carbon ionic liquid electrode

Ke-Jing Huang [a,b], De-Jun Niu [b], Jun-Yong Sun [b], Jun-Jie Zhu [a,*]

[a] Key Laboratory of Analytical Chemistry for Life Science (Ministry of Education of China), School of Chemistry and Chemical Engineering, Nanjing University, Nanjing 210093, PR China
[b] College of Chemistry and Chemical Engineering, Xinyang Normal University, Xinyang 464000, PR China

ARTICLE INFO

Article history:
Available online 11 January 2011

Keywords:
Amine-functionalized graphene
Gold nanoparticles
Carbon ionic liquid electrode
α-Fetoprotein
Immunosensor

ABSTRACT

A sensitive label-free amperometric immunosensor was developed based on the amine-functionalized graphene (GR-NH_2) and gold nanoparticles (AuNPs) composite modified carbon ionic liquid electrode (CILE). CILE was fabricated by using an ionic liquid of 1-octyl-3-methylimidazolium hexafluorophosphate as binder. The nanocomposite AuNPs/GR-NH_2 had prominent biocompatibility, good electron transfer ability, large specific surface area, and primarily excellent adsorption. The negatively charged AuNPs could be adsorbed on the positively charged GR-NH_2 modified CILE surface by electrostatic adsorption, and then to immobilize α-fetoprotein antibody (anti-AFP) for the assay of α-fetoprotein (AFP). The fabricated procedures and electrochemical behaviors of the immunosensor were characterized by electrochemical impedance spectroscopy (EIS) and cyclic voltammetry (CV). The anti-AFP/AuNPs/GR-NH_2 modified CILE was sensitive to AFP in linear relation between 1 and 250 ng mL^{-1} with the correlation coefficient of 0.995, and the detection limit ($S/N = 3$) was 0.1 ng mL^{-1} under the optimal conditions. In addition, the proposed immunosensor exhibited good sensitivity, selectivity, stability and long-term maintenance of bioactivity and it may be used to immobilize other biomoleculars to develop biosensor for the detection of other antigens or biocompounds.

1. Introduction

Cancer biomarkers are molecules occurring in blood or tissue, which are associated with cancer and whose measurement or identification plays an important role in patient diagnosis and clinical research [1,2]. α-Fetoprotein (AFP) is one of the most extensively used clinical cancer biomarkers [3]. Elevated AFP concentration in serum may be an early indication of some cancerous diseases such as hepatocellular cancer, liver metastasis from gastric cancer, testicular cancer, and nasopharyngeal cancer. Thus, the detection of AFP is absolutely necessary in clinical assay. Due to the specific binding of antibody to its antigen, immunoassays have recently gained increasing attention in the quantitative detection of cancer biomarkers [4,5]. Compared with conventional immunoassay techniques, immunosensors are of great interest because of their potential utility as specific, simple, label-free and direct detection techniques with advantages including reductions in size, cost, and time of analysis [6]. As one type of immunosensor, electrochemical immunosensors have attracted considerable interest due to their intrinsic advantages, such as high sensitivity, low cost, low power requirements and high compatibility with advanced micromachining technologies [7,8]. One key area of electrochemical immunosensors research is the use of various materials with nanoparticle like physical and chemical properties because they provide a large surface area and improve the biocompatibility, stability, and immobilization of biomolecules on the electrode surface [9,10].

Graphene is a flat monolayer of carbon atoms tightly packed into a two-dimensional honeycomb lattice. Recently, it has attracted considerable attention due to high electrical conductivity, high surface-to-volume ratio, high electron transfer rate, and exceptional thermal stability [11–13]. Some research effort has been made to explore its fascinating applications in fabricating various electrical devices, such as batteries [14], field-effect transistors [15], electrochemiluminescent sensor [16], electromechanical resonators [17] and electrochemical biosensors [18]. However, many of the interesting and unique properties of graphene can only be realized after it is integrated into more complex assemblies [19]. A useful technique to incorporate graphene into such assemblies is through chemical functionalization of the graphene, which enables chemical covalent bonding between the graphene and the material of interest. Functionalized graphene are easier to disperse in organic solvents and water, which can improve the dispersion

* Corresponding author. Fax: +86 25 83594976.
E-mail address: jjzhu@nju.edu.cn (J.-J. Zhu).

1572-6657/$ - see front matter © 2011 Elsevier B.V. All rights reserved.
doi:10.1016/j.jelechem.2011.01.007

and homogeneity of the graphene within the polymer and yield novel types of electrically conductive nanocomposites [20,21].

In the present work, a novel electrochemical immunosensor was designed based on amino-functionalization graphene sheets (GR-NH_2) and gold nanoparticles (AuNPs) composite modified carbon ionic liquid electrode (CILE). AuNPs is a kind of well known bio-nanomaterials because of their large specific surface area, strong adsorption ability, well suitability and good conductivity [22,23]; it can strongly interact with biomaterials and has been utilized as a intermediator to immobilize antibody to efficiently retain its activity and to enhance current response in the construction of a sensitive amperometric immunosensor. Therefore, it has drawn much attention in constructing electrical sensors such as DNA-AuNPs assemblies [24], enzymes biosensors [25] and immunosensors [26]. Recently, room temperature ionic liquids (RTIL) are more and more explored as a new kind of modifier to make an ionic liquid modified carbon paste electrode because they can provide a remarkable increase in the electron transfer rate of different organic and/or inorganic electroactive compounds and offer a marked decrease in the overpotential for biomolecules and enhance the electrochemical signal. In order to further improve the performance of the immunosensor, AuNPs and carbon ionic liquid electrode (CILE) was applied in the construction of the present immunosensor. The preparation, characterization, optimal conditions, and preliminary analysis of real samples for the detection of AFP were investigated in detail. It showed that AuNPs/graphen-NH_2 nanocomposite could effectively facilitate the direct electron transfer of $Fe(CN)_6^{3-/4-}$ to the electrode, and thus greatly improve the sensitivity of the immunosensor. This developed biosensor showed good performances, such as high sensitivity, improved stability, good selectivity and wide linear range owing to the synergic effects of graphen-NH_2, AuNPs and CILE. This strategy could be further developed for practical clinical detections of AFP and other important tumor markers.

2. Experimental

2.1. Materials

Chloroauric acid, sodium citrate, iron chloride hexahydrate, potassium ferricyanide graphite powder, hydrazine solution (50 wt.%) and ammonia solution (28 wt.%) was obtained from Shanghai Chemical Reagent Corporation (Shanghai, China). Bovine serum albumin (BSA), $SOCl_2$ and $NH_2(CH_2)_2NH_2$ were obtained from Sigma (Saint Louis, MO, USA). Anti-AFP and AFP were purchased from Biocell Company (Zhengzhou, China). 1-octyl-3-methylimidazolium hexafluorophosphate ($OMIMPF_6$) was obtained from Chengjie Chemical Co., Ltd. (Shanghai, China). Phosphate-buffered saline (PBS, 0.01 M) at various pH values was prepared by mixing a stockstandard solution of KH_2PO_4 and K_2HPO_4, which was used as the measuring buffer, and then adjusting the pH with 0.1 M KOH and H_3PO_4. Gold nanoparticles were produced by reducing gold chloride tetrahydrate with citric acid at 100 °C for half an hour [27]. The mean size of the prepared Au colloids was about 20 nm. The AFP was stored in the frozen state, and its standard solutions were prepared daily as in use. Serum samples provided by Xinyang Central Hospital (Xinyang, China) were stored at 4 °C in a freezer. All other chemicals were of analytical grade and used without further purification. Ultrapure water (18.2 MΩ) was obtained from a Milli-Q water purification system and used throughout.

2.2. Instruments

CHI660A electrochemical workstation (CH Instruments, USA) and a standard three-electrode cell contained a platinum wire auxiliary electrode, a saturated calomel reference electrode (SCE) and the modified electrode as working electrode were employed for electrochemical studies. All potential values given below refer to SCE. FT-IR spectroscopy was obtained using Bruker Tensor 27 Spectrometer (Germany). Scanning Electron Microscopy (SEM) measurement was carried out by JSM-6700 F Scanning Electron Microscope (JEOL Ltd., Japan).

2.3. Preparation of GR-NH_2

Graphene oxide was prepared from graphite according to Hummers and Offeman method. The graphene oxide was firstly washed with HCl solution (5%, v/v), and then repeatedly washed with water until the pH of filtrate was neutral. Through extremely rapid heating and successful splitting of graphite oxide, wrinkled graphene sheets functionalized with hydroxyl and carboxylic groups were obtained. The resultant product was then chlorinated by refluxing for 12 h with $SOCl_2$ at 70 °C. After evaporating any remaining $SOCl_2$, GR-NH_2 were obtained by reaction with $NH_2(CH_2)_2NH_2$ in dehydrated toluene for 24 h at 70 °C. After washing with ethanol and deionized water several times, GR-NH_2 powder was obtained from drying at 50 °C in vacuum for 24 h.

2.4. Fabrication of the immunosensor

The CILE was fabricated with the following procedures: graphite powder and $OMIMPF_6$ (4:1, w/w) were mixed in a mortar until a homogeneous paste was obtained. The prepared carbon paste was tightly packed into a PVC tube (internal diameter of 3 mm) and a cope wire was introduced into the other end for electrical contact. Prior to use, the surface of the electrode was smoothed with a weighing paper. For electrode preparation, 1 mg of GR-NH_2 was dispersed in 1 mL of water using an ultrasonic bath to give a black suspension. After carefully washed with water, the CILE was treated by dropping 10 μL of GR-NH_2 suspension and then dried in air. The prepared GR-NH_2/CILE was immersed in AuNPs solution and left for 10 h to adsorb a layer of AuNPs on electrode surface. After rinsed with water, the immobilization of anti-AFP to AuNPs was accomplished by immersing the resultant electrode in anti-AFP solution at 4 °C for 12 h, and then the antibody-modified electrode was thoroughly washed with PBS. At last the resulting electrode was incubated in BSA solution (w/w, 0.25%) for 2 h in order to block possible remaining active sites and avoid the nonspecific adsorption. After the modified electrode was washed carefully with PBS, an immunosensor was fabricated and stored at 4 °C when not in use. Schematic illustration of the stepwise preparation process of the immunosensor was shown in Scheme 1.

2.5. Electrochemical measurements

Electrochemical impedance spectroscopy measurements were carried out in the presence of 5 mM $Fe(CN)_6^{3-/4-}$ as a redox probe in PBS (pH 7.0). The alternative voltage was 5 mV and the frequency range is 0.1–10 kHz.

The electrochemical characteristics of the modified electrode were characterized by cyclic voltammetry (CV). Electrochemical measurements were done in a conventional electrochemical cell. CV scans were taken from −0.2 to 0.6 V (versus SCE) with a scan rate of 50 mV s^{-1} in 5 mL PBS (pH 7.0). The amperometric detection was based on the variation of current response before and after immunoreaction. When the background current was stabilized, the current response was recorded as I_0. Due to the immunocomplex restraining the electron transfer, the current response of the immunosensor decreased to a minimum after the immunoreaction and was recorded as I. Therefore, the immunosensor current shift (ΔI) was given by $\Delta I = I_0 - I$.

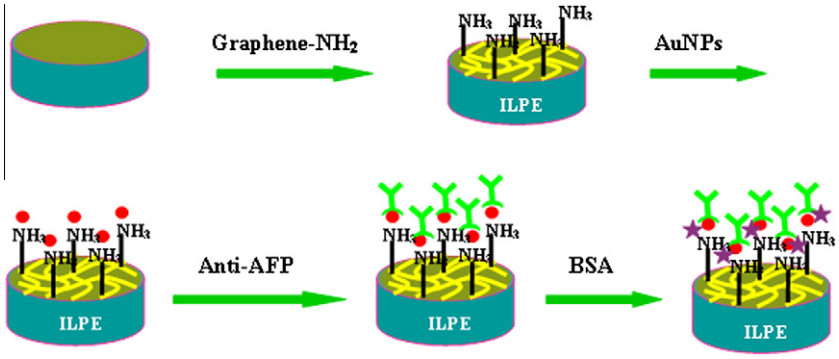

Scheme 1. The stepwise fabrication process of the immunosensor.

3. Results and discussion

3.1. Morphological characterization of GR-NH_2–AuNPs composite

In this paper, the electrochemical immunosensor was fabricated using the AuNPs/GR-NH_2 composite film as matrix. Addition of GR-NH_2 was expected to improve the conductivity and enhance the immobilized capacity toward biomolecules of the base electrode, which was favor to electron communication between the biomolecules and the base electrode. So the as-prepared GR-NH_2 and AuNPs/GR-NH_2 composite should be characterized.

The surface morphologies of GR-NH_2 and AuNPs/GR-NH_2 composite were examined by SEM observation. The top views of GR-NH_2 clearly illustrated the typically flakelike with slightly scrolled edges shapes (Fig. 1a). Fig. 1b presented the SEM image of AuNPs/GR-NH_2 composite. It was obviously showed that a layer of compact AuNPs was formed on the GR-NH_2 surface. AuNPs were compactly embedded on the GR-NH_2 substrate. It was worth notice that, as shown in the SEM images, the as-prepared GR-NH_2 nanoparticles exhibited considerable edge plane defect structures. These edge plane defects have shown to be essentially responsible for the high electron transfer kinetics and the electrocatalytic activity of graphene which contributes significantly to the electrochemical property of the present GR-NH_2 nanocomposite as well [28,29].

The as-prepared GO, GR and GR-NH_2 was characterized with FT-IR spectroscopy, as shown in Fig. 2. In the FT-IR spectrum of GO (Fig. 1c), we observe a strong and broad absorption at 3421 cm^{-1} due to O—H stretching vibration. The C=O stretching of COOH groups situated at edges of GO sheets is observed at 1722 cm^{-1}. The absorptions due to the O—H bending vibration, epoxide groups and skeletal ring vibrations are observed around 1626 cm^{-1}. The absorption at 1384 cm^{-1} may be attributed to tertiary C—OH groups. The IR spectrum in Fig. 1d confirms reduction of GO sheets. Here the absorption due to the C=O group (1722 cm^{-1}) is decreased very much in intensity and absorptions at 1626 and 1384 cm^{-1} are absent, suggesting the considerable deoxygenation by the chemical reduction process. Fig. 1e showed the IR spectrum of GR-NH_2. A corresponding appearance of a band with lower frequency (1638 cm^{-1}) assigned to the amide carbonyl (C=O) stretch. The NH_2 stretch band appears at 3395 cm^{-1}. The small 3296 cm^{-1} peak may be due to the NH_2 symmetric stretch of the amine group. In addition, the presence of new bands at 1594 and 1280 cm^{-1}, corresponding to N—H in-plane and C—N bond stretching, respectively, further confirms the presence of the amide functional group.

3.2. Electrochemical characterization of the immunosensor

All electrochemical measurements were performed in PBS (pH 7.0) containing 0.1 M KCl and 5 mM $Fe(CN)_6^{3-/4-}$. The CV of ferricyanide was chosen as a marker to investigate the changes of the electrode behavior before and after each assembly step. Fig. 2 shows the CV of $Fe(CN)_6^{3-/4-}$ at the AuNPs/GR-NH_2/CILE (curve a), GR-NH_2/CILE (curve b), bare CILE (curve c), AFP/AuNPs/GR-NH_2/CILE (curve d), BSA/anti-AFP/AuNPs/GR-NH_2/CILE (curve e), and AFP/BSA/anti-AFP/AuNPs/GR-NH_2/CILE (curve f), respectively. As shown in Fig. 2A, it was observed that the peak current of GR-NH_2/CILE greatly increased after the modification of GR-NH_2. Obviously, the GR-NH_2 film increased the conductivity and stability of GR-NH_2/CILE. Modification of AuNPs increases the conductivity of the GR-NH_2/CILE film, resulting in the increase of the anodic peak and cathodic peak currents as AuNPs acts as a conducting wire or an electron communication relay, which increased the electron-transfer efficiency [30]. When the modified electrode was incubated with anti-AFP, the redox peak currents decreased significantly, because the immobilized protein acted as insulator blocking the electron communication of the probe with the electrode. Peak current decreased in the same way after BSA was used to block non-specific sites. After AFP molecules specifically recognized with the immobilized antibody, the redox peak currents of $Fe(CN)_6^{4-/3-}$ decreased further, indicating the formed immunocomplex might further hinder the electron-transfer pathway of the ferricyanide.

Electrochemical impedance spectroscopy (EIS) can give the information about the stepwise assembly of the immunosensor based on the impedance changes of the electrode surface. In EIS, the semicircle diameter equals the electron-transfer resistance (*R*et). Fig. 3 shows the impedance spectra corresponding to the stepwise modification processes. The data can be fitted with a modified Randles equivalent circuit (inset in Fig. 3). It was observed that the EIS of the CILE (curve a), GR-NH_2/CILE (curve b) and AuNPs/GR-NH_2/CILE (curve c) displayed an almost straight line in the Nyquist plot of impedance spectroscopy, characteristics of a diffusion-limited electron-transfer process. Especially, the electron-transfer resistance (*R*et) of the GR-NH_2/CILE and AuNPs/GR-NH_2/CILE showed more little value than that of CILE, indicating that the conductivity of the GR-NH_2 and AuNPs mediator were essentially beneficial to the electron transfer. However, when anti-AFP (curve d) and BSA (curve e) were immobilized onto AuNPs/GR-NH_2/CILE, the resistances for the modified electrode increased gradually, which were caused by the nonconductive properties of anti-AFP and BSA which acted as an inert electron layer and retarded the electron transfer. After the prepared immunosensor was incubated with AFP antigen solution (curve f), a larger increase of the resistance was shown.

3.3. Influence of the scan rate

Typical CV curves of the AFP/BSA/anti-AFP/AuNPs/GR-NH_2/CILE in 0.1 M PBS at different scan rates were shown in Fig. 4. It can be seen that a pair of roughly symmetric anodic and cathodic peaks appeared with almost equal peak currents in the scan rate range

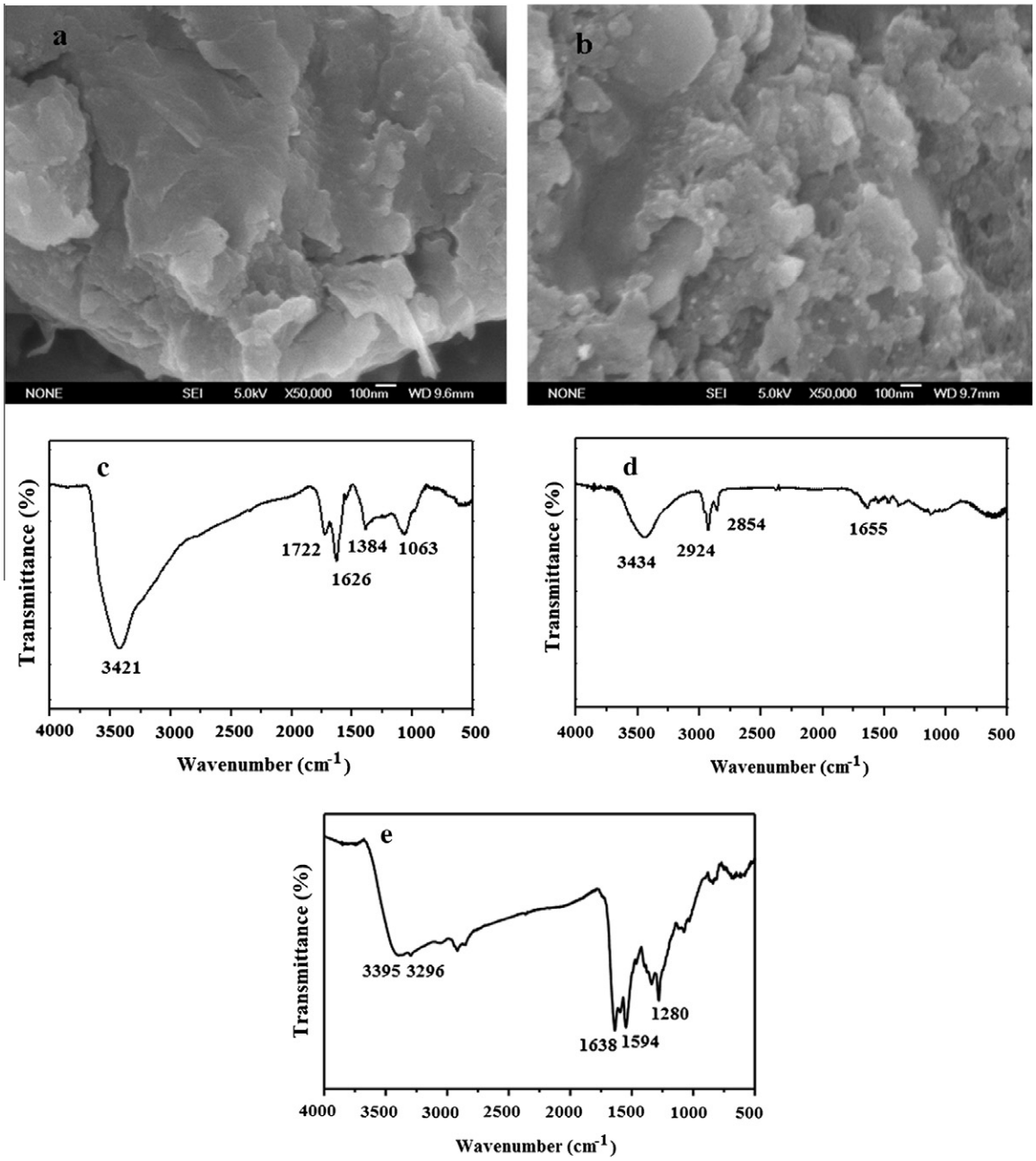

Fig. 1. (a) SEM images of GR-NH_2. (b) SEM images of AuNPs/GR-NH_2. (c) FT-IR spectra of GO. (d) FT-IR spectra of GR. (e) FT-IR spectra of GR-NH_2.

from 0.05 to 0.50 V s^{-1}. The peak-to-peak separation also increased with the scan rate. A good linear relationship was found for the peak current and scan rate, with the results shown in Fig. 4 (upper right inset). The reduction and oxidation peak currents rise linearly with the linear egression equations as $i_{pc} = 1.127v^{1/2} - 9.066$ ($R = 0.994$), $i_{pa} = -7.589v^{1/2} - 4.358$ ($R = 0.989$), respectively, suggesting that the reaction is quasi-reversible diffusion-controlled behavior with an electron transfer process.

3.4. Optimization of experimental conditions

The experimental conditions, which can affect the amperometric determination of AFP, including the pH of supporting electrolyte, the incubation temperature and time of immunoreaction, were optimized.

The pH of the measuring solution may affect the immunosensor response signals. Because unsuitable pH not only may cause protein denaturalization, but also affect the affinity between the protein and the electrode surface. The effect of pH on the immunosensor in the pH range of 4.0–9.0 was evaluated. The results showed the current response reached the minimum at pH 7.0, and then the current response increased if the pH higher or lower than this value. The reason may be that, the higher and lower pH may damage the protein and affect the lifetime of the immunosensor. So, the pH 7.0 was used for further experiments.

The effect of the temperature is important on the activity of the antigen and antibody. The effect of the temperature was studied from 10 to 50 °C. It was found that the current response decreased with the increasing temperature up to 37 °C. However, temperatures over 40 °C caused irreversible behavior (denaturation of proteins) involved in the process. Thus, 37 °C was employed as the optimum incubation temperature.

The immunochemical incubation time was another influence condition of the immunosensor. When the analyte antigens

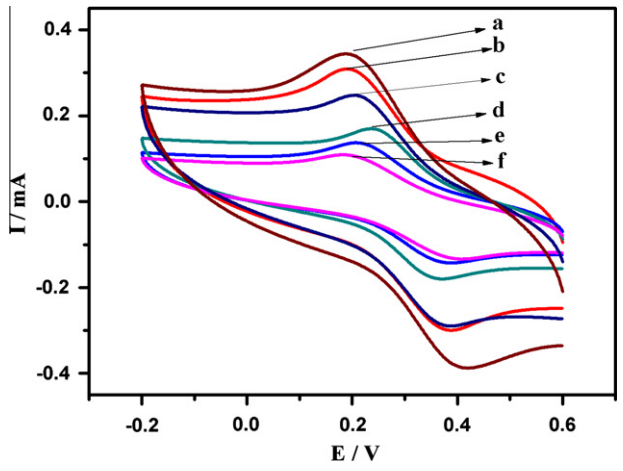

Fig. 2. Cyclic voltammograms of different modified electrodes in pH 7.0 PBS containing 0.1 M KCl: (a) AuNPs/GR-NH_2/CILE, (b) GR-NH_2/CILE, (c) bare CILE, (d) AFP/AuNPs/GR-NH_2/CILE, (e) BSA/anti-AFP/AuNPs/GR-NH_2/CILE, and (f) AFP/BSA/anti-AFP/AuNPs/GR-NH_2/CILE.

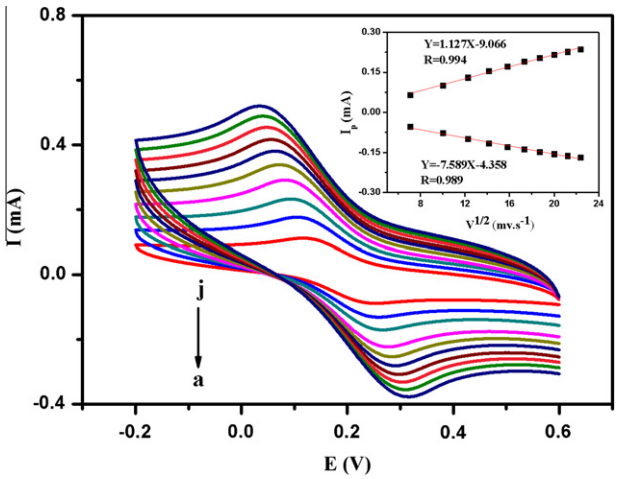

Fig. 4. CVs of the immunosensor in pH 7.0 PBS containing 0.1 M KCl and 5.0 mM $Fe(CN)_6^{4-/3-}$ at the different scan rate of (from inner to outer): 50, 100, 150, 200, 250, 300, 350, 400, 450, 500 mV s^{-1}. The inset shows the linear relationship between the peak currents and the square root of scan rate.

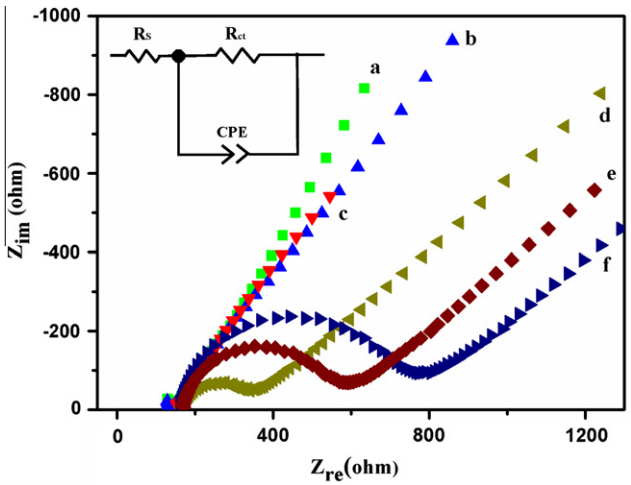

Fig. 3. Nyquist plots of the different electrodes in a PBS solution containing 0.1 M KCl and 5.0 mM $Fe(CN)_6^{4-/3-}$: (a) CILE, (b) GR-NH_2/CILE, (c) AuNPs/GR-NH_2/CILE, (d) anti-AFP/AuNPs/GR-NH_2/CILE, (e) BSA/anti-AFP/AuNPs/GR-NH_2/CILE, (e) BSA–anti-HIgG/AuNPs/APS/PB/CILE, and (f) AFP/BSA/anti-AFP/AuNPs/GR-NH_2/CILE. The frequency range was from 0.1 to 100,000 Hz with perturbation amplitude of 5 mV. Inset: equivalent circuit for fitting the plots. *Rs*: solution resistance; *Rct*: charge-transfer resistance; CPE: constant phase element, which is a complex of various elements.

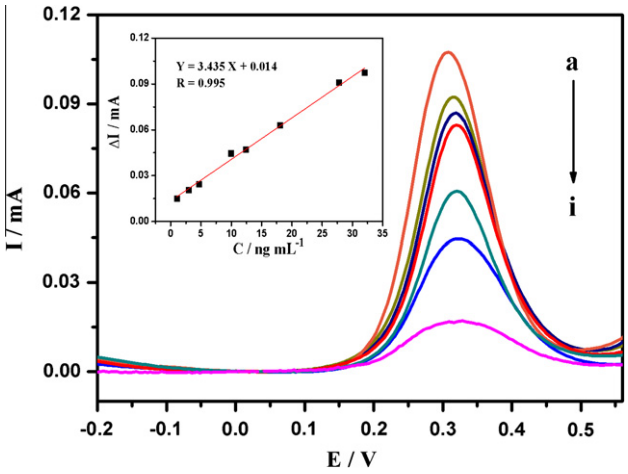

Fig. 5. DPV curves of the immunosensor after incubating with various concentrations of AFP: (a) blank solution, curves b–i represent 8, 24, 35, 70, 94, 140, 218, and 250 ng mL^{-1} AFP (from top to bottom). Inset: calibration curve of the immunosensor for AFP determination.

reached the antibodies modified on the surface of the immunosensor, it would take some time for the contracting species to form immunocomplexes. The influence of the immunochemical incubation time of the immunosensor on the response signals was investigated in the range of 10–60 min. With increasing of the incubation time, the peak current rapidly decreased and after 30 min the current reached a steady state, indicating the antigen molecules in the solution were completely captured by the immobilized antibody molecules. Therefore, the incubation time of 30 min was used in the subsequent work.

3.5. Analytical performance

Under the optimization of experimental conditions, the developed immunosensor was exposed to various concentrations of AFP solutions. After the antigen reacted with the antibody immobilized on the electrode, a DPV curve was collected (Fig. 5). As expected, the current response signal decreased with increase in AFP concentration. It could be understood that more AFP could bind to the immobilized antibodies at higher concentrations of antigens, and the antigen–antibody complex acted as an inert kinetic barrier for the electron-transfer of the mediator of ferricyanide. As a result, the amperometric response decreased with increase of the AFP concentration. As presented in Fig. 5, the amperometric response increased with the increase of AFP concentration from 1 to 250 ng mL^{-1} with a correlation coefficient of 0.995. The regression equation was $Y = 3.435X + 0.014$ (Y is the change in current response signal before and after the antigen–antibody reactions). The detection limit was estimated to be 0.1 ng mL^{-1} based on a signal to noise ratio of 3. The detection limit of this immunosensor was better than those of previously reported AFP immunosensors based on carbon nanotube/gold nanoparticle doped chitosan film (0.6 ng mL^{-1}) [31], CdS nanoparticles and thionine bilayer films (0.12 ng mL^{-1}) [32], and phenylboronic acid monolayer on gold (40 ng mL^{-1}) [33].

Table 1
Comparison of AFP levels determined using proposed method and ELISA.

Serum samples	1	2	3	4	5
Immunosensor (ng mL^{-1}, $n = 6$)	15.2	34.1	56.5	102.8	138.6
ELISA (ng mL^{-1}, $n = 6$)	14.3	32.1	59.8	111.3	131.0
Relative deviation (%)	6.3	6.2	−5.5	−7.6	5.8

3.6. Precision, selectivity and stability

The precision of the immunosensors was investigated by using the variation coefficients (CVs) of intra- and inter-assays. The intra-assay precision of the analytical method was evaluated by analyzing four concentration levels six times per run. The CVs of intra-assay were 4.6%, 4.4%, 5.1% and 4.5% at 1, 10, 100, and 250 ng mL^{-1} of AFP, respectively. Similarly, the CVs of the inter-assay were 5.6, 6.1, 6.4, and 5.2% at 1, 10, 100, and 250 ng mL^{-1} of AFP, respectively. Thus, the precision and reproducibility of the immunosensors was acceptable.

To monitor the differences in response of the immunosensor to interference degree or crossing recognition level, carcinoembryonic antigen, low density lipoprotein and prostate-specific antigen with various concentrations were added into the detection system, respectively. The interference degree of variability between different proteins was 3.2–6.5%. Therefore, the selectivity of the developed immunosensor was acceptable.

The stability of the developed immunosensor was examined. When not in use, they could be stored in pH 7.0 PBS at 4 °C for at least 2 weeks without obvious signal change (signal change below 5%). Moreover, it retained 93.4% of its initial response after a storage period of 20 days. We speculate that the slow decrease of response mainly attributed to the gradual deactivation of the immobilized biomolecules on the surface of the nanoparticles.

3.7. Real sample analysis

To monitor the analytical reliability and possible application of the developed immunosensor, five serum samples were assayed using the developed immunosensor, and the results were then compared with the reference values obtained by the standard ELISA. The results are summarized in Table 1. It showed that both results were in acceptable agreement. The absolute value of relative errors of the results acquired by two methods was lower than 8.0%. So, the developed immunosensor provides a possible application for the detection of AFP in clinical diagnostics.

4. Conclusions

In the present work, a novel strategy of an amperometric immunosensor for AFP has been proposed based on the antigen adsorbed in AuNPs/GR-NH_2/CILE. The immunosensor could be used for determining the serum AFP level indirectly. The combination of the good conductivity of RTIL and GR-NH_2, and the advantages of the AuNPs, including biocompatibility and amplification, enhanced the sensitivity of the immunosensor significantly. The biosensor possesses good bioactivity, comparable detection limit and linear range, and acceptable storage stability. The results showed that the method was simple and sensitive enough for determination of AFP in human serum samples with good precision and accuracy. This flexible immunosensor could be extended to the application of other antigens or other bioactive molecules.

Acknowledgments

This work was supported by National Natural Science Foundation of China (20805040 and 20635020), Excellent Youth Foundation of He'nan Scientific Committee (104100510020), China Postdoctoral Science Foundation funded project (200902508 and 20080430163), Jiangsu Planned Projects for Postdoctoral Research Funds (0801041B), and sponsored by Program for Science & Technology Innovation Talents in Universities of Henan Province (2010HASTIT025).

References

[1] M. Miyake, K. Sugano, H. Sugino, K. Imai, E. Matsumoto, K. Maeda, S. Fukuzono, Y. Hirao, Cancer Sci. 101 (2010) 250–258.
[2] B. Zhang, X. Zhang, H.H. Yan, S.J. Xu, D.H. Tang, W.I. Fu, Biosens. Bioelectron. 23 (2007) 19–25.
[3] X.W. Wang, H. Xie, Life Sci. 64 (1999) 17–23.
[4] F. Gas, B. Baus, L. Pinto, C. Compere, V. Tanchou, E. Quemeneur, Biosens. Bioelectron. 25 (2010) 1235–1239.
[5] W. Bosker, M. Huestis, Clin. Chem. 55 (2009) 1910–1931.
[6] Z. Dai, F. Yan, H. Yu, X.Y. Hu, H.X. Ju, J. Immunol. Methods 287 (2004) 13–20.
[7] U. Lad, S. Khokhar, G. Kale, Anal. Chem. 80 (2008) 7910–7917.
[8] H. Zhang, Q. Zhao, X. Li, X. Le, Analyst 132 (2007) 724–737.
[9] J.S. Li, Z.S. Wu, H. Wang, G.L. Shen, R.Q.A. Yu, Sens. Actuators B 110 (2005) 327–335.
[10] S.E. Moulton, J.N. Barisci, A. Bath, R. Stella, G.G. Wallace, Langmuir 21 (2005) 316–322.
[11] C. Shan, H. Yang, D. Han, Q. Zhang, A. Ivaska, L. Niu, Biosens. Bioelectron. 25 (2010) 1070–1074.
[12] A. Savchenko, Science 323 (2009) 589–590.
[13] D. Li, R. Kaner, Science 320 (2008) 1170–1171.
[14] T. Cassagneau, J.H. Fendler, Adv. Mater. 10 (1998) 877–881.
[15] S. Gilje, S. Han, M. Wang, K.L. Wang, R.B. Kaner, Nano Lett. 7 (2007) 3394–3398.
[16] L.Z. Hu, G.B. Xu, Chem. Soc. Rev. 39 (2010) 3275–3304.
[17] J.S. Bunch, A.M. Van der Zande, S.S. Verbridge, I.W. Frank, D.M. Tanenbaum, J.M. Parpia, H.G. Craighead, P.L. McEuen, Science 315 (2007) 490–493.
[18] M.H. Yanga, A. Javadib, H. Lia, S.Q. Gong, Biosens. Bioelectron. 26 (2010) 560–565.
[19] C.L. Fu, W.S. Yang, X. Chen, D.G. Evans, Electrochem. Commun. 11 (2009) 997–1000.
[20] S. Stankovich, D.A. Dikin, G.H.B. Dommett, K.M. Kohlhaas, E.J. Zimney, E.A. Stach, R.D. Piner, S.T. Nguyen, R.S. Ruoff, Nature 442 (2006) 282–286.
[21] G. Eda, M. Chhowalla, Nano Lett. 9 (2009) 814–818.
[22] Z.M. Liu, Y. Yang, H. Wang, Y.L. Liu, G.L. Shen, R.Q. Yu, Sens. Actuators B 106 (2005) 394–400.
[23] Y. Xiao, F. Patolsky, E. Katz, J.F. Hainfeld, I. Willner, Science 299 (2003) 1877–1881.
[24] W.J. Parak, T. Pellegrino, C.M. Micheel, D. Gerion, S.C. Williams, A.P. Alivisatos, Nano Lett. 3 (2003) 33–36.
[25] A. Gole, C. Dash, C. Soman, S.R. Sainkar, M. Rao, M. Sastry, Bioconjugate Chem. 12 (2001) 684–690.
[26] S.H. Chen, R. Yuan, Y.Q. Chai, Y. Xu, L.G. Min, N. Li, Sens. Actuators B 135 (2008) 236–244.
[27] G. Frens, Phys. Sci. 241 (1973) 20–22.
[28] D. Chen, L. Tang, J. Li, Chem. Soc. Rev. 39 (2010) 3157–3180.
[29] M. Pumera, Chem. Soc. Rev. 39 (2010) 4146–4157.
[30] H. Chen, J.H. Jiang, Y. Huang, T. Deng, J.S. Li, G.L. Shen, R.Q. Yu, Sens. Actuators B 117 (2006) 211–218.
[31] J.H. Lin, C.Y. He, L.J. Zhang, S.S. Zhang, Anal. Biochem. 384 (2009) 130–135.
[32] X.M. Miao, R. Yuan, Y.Q. Chai, Y.T. Shi, Y.R. Yuan, Biochem. Eng. J. 38 (2008) 9–15.
[33] Z. Wang, Y.F. Tu, S.Q. Liu, Talanta 77 (2008) 815–821.